Pakistan J. Zool., pp 1-13, 2026. **DOI**: https://dx.doi.org/10.17582/journal.pjz/20260421043057

Identification and Characterization of Phytochemicals from *Fumaria indica* as Potential NRF2 Inhibitors

Sadia Zahoor[1], Muhammad Abrar-ul-Haq[1], Nabia Fayyaz[1], Amara Maryam[1], Muhammad Haroon Hamed[2], Muhammad Khan[1]*, Muhammad Irfan[3] and Muhammad Akhtar Ali[4]*

[1]*Cancer Research Lab, Institute of Zoology, University of the Punjab, Lahore*
[2]*Department of Zoology, Wildlife and Fisheries, University of Agriculture, Faisalabad*
[3]*Department of Biotechnology. University of Sargodha, Sargodha*
[4]*School of Biological Sciences, University of the Punjab, Quaid e Azam Campus, Lahore*

Check for updates

ABSTRACT

NRF2 is an essential transcription factor, which is involved in the regulation of redox balance and many other cellular processes including cell growth and division. It is over-activated in numerous types of cancers and therefore, considered a key drug target in cancer treatment. This research was conducted to identify the bioactive molecules of *Fumaria indica* as potential NRF2 inhibitors by virtual screening. Molecular docking study was done with PyRX. The compounds with the highest binding energies were ranked and the ten highest ranked compounds were chosen for further analysis. The binding interactions of these compounds with NRF2 were also illustrated with virtual tools such as PyMOL, Biovia Discovery Studio, and Ligplot+. The dissociation constants were computed and Ki values were obtained and plotted against binding energies. According to the binding energy and protein-ligand interactions, narlumidine and coclaurine were identified as the most potent NRF2 inhibitors. The stability and compactness of narlumidine-NRF2 and coclaurine-NRF2 complexes were further confirmed by molecular dynamics (MD) simulations carried out with GROMACS software, with narlumidine being more effective. Drug-likeness properties were evaluated using Radar plots through ADMET lab 2 and a more comprehensive analysis was done using ADMET lab 3 to check the therapeutic potential of top two hit compounds. Both compounds exhibit drug likeness and excellent physicochemical properties. These results revealed narlumidine and coclaurine as a possible NRF2 inhibitor and therapeutic agent. Moreover, we have also evaluated the anticancer activity of *Fumaria indica* alcoholic extract through MTT essay. Increasing concentrations of extract treatment produced effects on cell viability that were dose-dependent. IC_{50} value was found to be about 53.95 mM indicating somewhat toxic activity. Further experimental studies are suggested to confirm the NRF2 antagonistic potential of narlumidine and coclaurine.

Article Information
Received 21 April 2026
Revised 25 June 2026
Accepted 10 July 2026
Available online 11 November 2026 (early access)

Authors' Contribution
MK designed and supervised the study. SZ performed experimental work and wrote initial draft. MAA, AM, MI, MHH, NF and MAH assisted in experimental work. MK edited and approved the manuscript.

Key words
***Fumaria indica*, NRF2 inhibitors, Narlumidine, Coclaurine, Molecular docking, Anticancer**

Online First Article

INTRODUCTION

Nuclear factor erythroid 2-related factor 2 (NRF2) is a crucial transcription factor involved in the regulation of antioxidant response and cellular redox homeostasis. Molecularly, NRF2 is encoded by 1816 base pairs and consists of 605 amino acids and seven conserved domains called NRF2-ECH homology (NEH) domains. They make it versatile in its functional responsibilities. For example, NEH1 domain has leucine zipper that helps in binding of NRF2 to small Maf proteins and DNA sequences called antioxidant response elements (ARE), which leads to transcription of target genes (George *et al*., 2022). The NEH2 domain is important for the binding of NRF2 to Keap1, a protein that targets NRF2 for degradation through ubiquitination. Other domains are NEH3, NEH4, NEH5, NEH6, and NEH7, which are involved in the regulation of the transcriptional activation of cytoprotective genes by NRF2, as well as in the regulation of the stability of NRF2 and its ability to interact with other molecules (George *et al*., 2022; Jaramillo and Zhang, 2013; Chowdhry *et al*.,

* Corresponding author: mkhan.zool@pu.edu.pk, akhtaralimuhammad@gmail.com
0030-9923/2026/0001-0001 $ 9.00/0

Copyright 2026 by the authors. Licensee Zoological Society of Pakistan.
This article is an open access article distributed under the terms and conditions of the Creative Commons Attribution (CC BY) license (https://creativecommons.org/licenses/by/4.0/).

2012). The 3D structure and various domains of NRF2 has been shown in Figure 1.

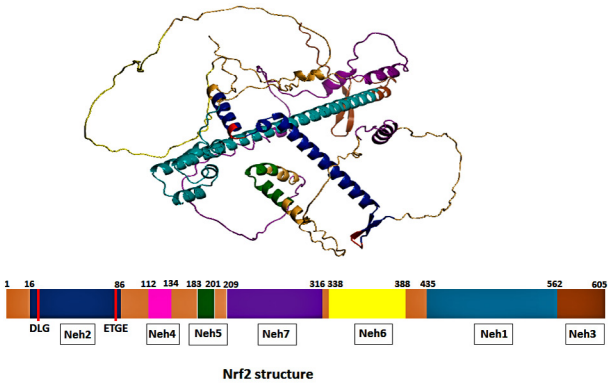


Fig. 1. 3D and linear structure of NRF2 protein, where color scheme represents each domain.

Under normal physiological conditions, the activation of NRF2 is kept at a check to avoid overactivation. It is mainly regulated by Keap1 which ensures that it is constantly degraded when the cell is not under stress. Under oxidative stress, certain cysteine residues on Keap1 are modified and therefore NRF2 is liberated. Free NRF2, therefore, translocate to the nucleus and interacts with AREs to promote the transcription of genes that are involved in antioxidant signal, detoxification, and cell repair mechanisms. This carefully controlled response helps in maintaining cellular health and prevents damage from reactive oxygen species (ROS) (Jaramillo and Zhang, 2013).

Nevertheless, the constant overactivation of NRF2 is problematic, especially in cancer-related cases. NRF2 is constitutively upregulated in many types of cancers, such as lung cancer, breast cancer, and ovarian cancer, and it enhances tumor growth, survival, and chemoresistance (Bellezza *et al*., 2018; Hayes and Dinkova-Kostova, 2014). This continuous activation can enable the cancer cells to subvert the protective effects of NRF2 and hence promote their growth and survival in the presence of therapies. As a result, NRF2 overactivation contributes to the development of aggressive, treatment-resistant tumors, making it a critical target in cancer therapy (Chowdhry *et al*., 2012). So, NRF2 inhibition is a promising target to treat different types of cancer (DeNicola *et al*., 2011).

Indeed, several NRF2 inhibitors have been developed and used in preclinical models but these were found to be associated with several challenges including nonselective, side effects and poor solubility. Moreover, the complexity of NRF2's involvement in different cellular processes makes it challenging to selectively target the protein for therapeutic purposes; if NRF2 is suppressed, other critical cellular processes may be affected and lead to adverse effects (Ackova *et al*., 2023; Banik *et al*., 2022; Sood *et al*., 2024; Zhang *et al*., 2023). These challenges underscore the necessity for developing new NRF2 inhibitors that are more specific, effective, and safe.

Natural products have played and continue to play a key role in drug discovery against a wide range of human diseases including cancer. It is estimated that about 60% anticancer drugs have been derived from natural sources including medicinal plants which make the major fraction of medicinal flora. It is fact that nature's created vast and diverse natural bioactive compounds library is matchless and exhibits tremendous biological and pharmacological activities. It is therefore logical to explore nature's made bioactive compound library to find HITS (Khan *et al*., 2015, 2016; Hassan *et al*., 2021) The present study was conducted to identify new novel NRF2 inhibitors from *Fumaria indica*, which has been shown to exhibit various biological and pharmacological properties (Gilani *et al*., 2005). The study entails virtual screening of phytochemicals from *Fumaria indica* for NRF2 inhibitors, molecular dynamic simulations and drug likeness analysis. Finally, we evaluated the anticancer activity of *Fumaria indica* extract by MTT assay.

MATERIALS AND METHODS

Compounds preparation

The compounds of *Fumaria indica* were downloaded in 3D SDF format from the IMPAAT database (IMPPAT, 2024). The structure of the NRF2 protein was modeled previously by our research group (Gul *et al*., 2025). Protein preparation was done by the Biovia Discovery Studio Visualizer. The process started by importing the protein structure in PDB format into Discovery Studio; all the water molecules and other heteroatoms were then eliminated for the purpose of the virtual environment that is suitable for docking studies. The purified interacting protein with NRF2 was free from other interacting molecules and was saved in PDB format. This prepared protein was then used for docking studies with the sixty compounds from *Fumaria indica*.

Screening of compounds

To identify potential compounds with effective binding affinity for the NRF2 protein active site, PyRx software was employed. The process commenced by importing the NRF2 protein structure in PDB format into PyRx and converting it to pdbqt format, which is optimized for docking studies. Subsequently, the 60 compounds from

Online First Article

Fumaria Indica were loaded into PyRx in SDF format. These compounds were converted to pdbqt format and underwent energy minimization. Docking simulations were executed by selecting "Run Vina > Start > Forward," with results stored in a CSV file.

Interaction analysis

The output from PyRx, which was stored in the mgl tools files, were visualized using PyMOL. The protein molecule in PDBQT format was then imported to PyMOL and the next was the PDBQT format file of each compound. First, the complex was presented in the form of a cartoon, and only states with the maximum number of hydrogen bonds were chosen. Other adjustment tools were then employed to analyze the protein residues that participated in the polar interactions with the complexes. The same procedure was followed for all the ten top hit compounds.

Likewise, the complexes of the NRF2 protein with each of the ten hit compounds were modeled in PyMOL and only the conformations with the highest number of hydrogen bonds were considered and the PDB files were produced. The complexes generated with PyMOL were then viewed with the help of LIGPLOT+ and Discovery Studio (2024). These top ten hit complexes were modeled separately to obtain their respective 2D images.

Calculation of inhibition constant

For each of the top 10 compounds, the predicted Ki values were calculated by substituting their respective ΔG binding energy values obtained from docking into the following formula:

Ki pred. = Exponential (ΔG/RT)

A graph was produced to compare the binding energies and Ki of top ten lead compounds. In the graph, compounds are shown on the X-axis, binding energy is shown on the right Y-axis and predicted Ki values on the left Y-axis.

MD simulation: GROMACS package

Among the narlumidine-NRF2 and coclaurine-NRF2 complexes with the highest negative binding energies and stable interactions, 100 ns MD simulations using GROMACS Development Team (2024) were performed to evaluate their stability in water. Compounds and proteins in the docking experiments were transformed from PDBQT to PDB using PyMOL and then to GROMOS using pdb2gmx which also created the topology file. The solute was placed in a cubic simulation box of dimensions $100 \times 100 \times 100$ Å by using the editconf module while SPC216 water was used for solvation. The system was balanced by replacing water molecules with ions as commanded by the genion command. Energy minimization was done using mdrun following preparation of a binary input file using grompp. To analyze the results after the simulation, various tools in GROMACS were employed including RMSD, RMSF, hydrogen bonds and radius of gyration (Astuti and Mutiara, 2009).

Drug likeness analysis

The drug-likeness properties of the top two hit compounds were predicted using ADMETLab 3. 0 (ADMET Lab 3, 2024), an online tool. Specific property data were studied and quantified in detail and were compared with their ideal values. Radar plots showing the physicochemical properties were created by using ADMET Lab 02.

Preparation of Fumaria indica *ethanolic extract*

The aerial parts of *Fumaria indica* were collected from University of the Punjab, New Campus Lahore and identified by an expert botanist. The plant aerial parts were shade-dried and coarsely crushed and extracted with 95% ethanol using Soxhlet extraction method and finally extract was evaporated to get crude extract as described previously (Khan *et al*., 2012).

Evaluation of anticancer activity

The DMEM containing 10% FBS and 1% penicillin-streptomycin was used to grow MCF-7 breast cancer cells at 37 ℃ in 5 % CO_2 incubator. Cells were seeded in 96-well plates in triplicates and allow to grow overnight. The cells were exposed to different concentrations of *Fumaria indica* extract for 24 h and MTT assay was applied to determine the cell viability as described previously (Mehmood *et al*., 2017). The stock solution of 20mM of plant extract was prepared by assuming the molecular mass of all compounds in extract roughly 500.

RESULTS

Binding energy and inhibition constant (Ki) of compounds of Fumaria indica

Virtual screening of the 60 compounds of *Fumaria indica* showed narlumidine and coclaurine as top two hit compounds, which have highest binding energy with the NRF2 protein. Top ten compounds with their binding energies and Ki constant are given in Table I. Graphical representation of relationship between Ki and binding energies have been shown in the Figure 2. Narlumidine and coclaurine exhibited the lowest Ki constant values, which showed their highest binding affinity with the NRF2 protein.

Online First Article

Table I. Compounds of *Fumaria indica* which exhibited top binding energies, with calculated inhibition constant(ki).

Ligands	Formula	Binding energy (Kcal/mol)	(Ki pred.) (µM)
Narlumidine	C21H19NO7	-8	1.29
Coclaurine	C17H19NO3	-7.7	2.1
Dihydrocoptisine	C19H15NO4	-7.3	4.23
8-Oxocoptisine	C19H13NO5	-7.3	4.23
Coptisine	C19H14NO4+	-7.2	5.01
Isorheagenine	C20H19NO6	-7.2	5.01
Norjuziphine	C17H19NO3	-7.2	5.01
Moupinamide	C18H19NO4	-7.2	5.01
Fumaramine	C21H20N2O5	-7.1	5.9
Lahorine	C20H14NO4+	-7	7.0

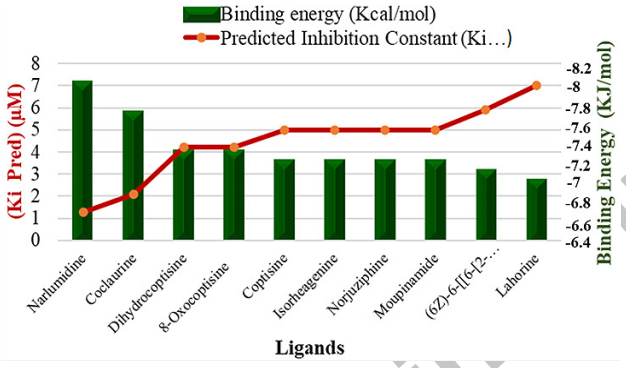


Fig. 2. Maximum binding energies and predicted K_i values of the top ten compounds of *Fumaria indica*.

Interaction of NRF2 with compounds of F. indica

Ten of the NRF2-compound complexes were further examined in terms of molecular interactions employing PyMOL, Discovery Studio, and LigPlot+. For the NRF2-narlumidine complex, hydrogen bonds and van der Waals interactions were observed and in addition, discovery studio and LigPlot+ suggested additional non-covalent and hydrophobic interactions particularly in ARG-43 that contributes to the stability of the complex (Fig. 3).The NRF2-coclaurine complex exhibited a significant hydrogen bonding with GLN-527 and GLU-47 and the presence of pi-pi and pi-alkyl interactions that were predicted in Discovery Studio was also confirmed by LigPlot+ analysis indicating the stability of the complex (Fig. 4). In the NRF2-Dihydrocoptisine complex, PyMOL and Discovery Studio found hydrogen bonds with TYR-46 and ARG-43 and hydrophobic interactions with ASP-530 as shown by LigPlot+ (Supplementary Fig. S1). The binding interactions between the NRF2-8-oxocoptisine complex were shown to involve multiple hydrogen bonds with ARG-43 and GLU-47, and Discovery Studio also showed that there were pi-cation, pi-anion, and pi-alkyl interactions, which were also supported by LigPlot+ (Supplementary Fig. S2). For the NRF2-coptisine complex, PyMOL and LigPlot+ identified hydrogen bonds between ARG-43 and O4 of coptisine and additional information about pi-pi, pi-alkyl, and pi-anion interactions in the complex were provided by Discovery Studio (Supplementary Fig. S3). In PyMOL, the NRF2-isorheagenine complex had hydrogen bonds with TYR-46 and GLN-527, with Discovery Studio showing additional alkyl and pi-anion interactions confirmed by LigPlot+, which showed isorheagenine selectivity (Supplementary Fig. S4). The NRF2-norjuziphine complex had three hydrogen bonds with TYR-46 and ARG-43 in PyMOL, whereas discovery Studio depicted pi-alkyl and pi-pi interactions and LigPlot+ further hydrogen bonds with ASP-534 and interaction stability and selectivity (Supplementary Fig. S5). The NRF2-moupinamide complex had three hydrogen bonds with TYR-46 and ARG-43, with further pi-alkyl and anionic interactions seen in Discovery Studio, LigPlot+ showing the details of these bonds prove that Moupinamide has a good binding affinity for NRF2

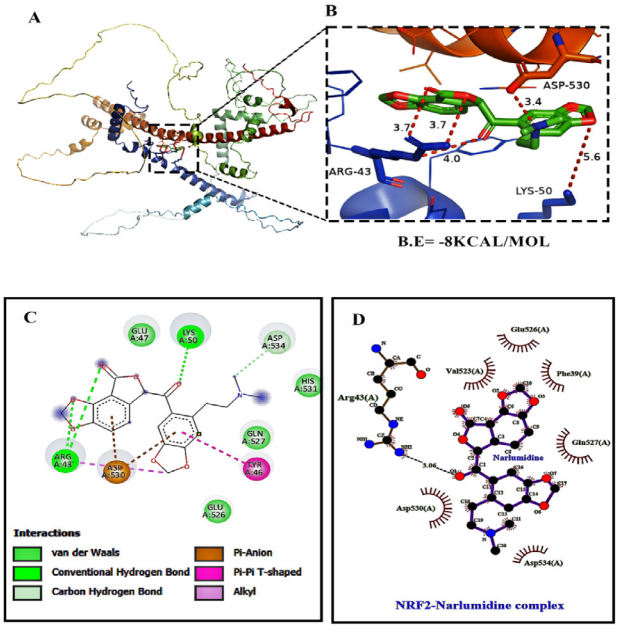


Fig. 3. Interaction analysis of NRF2-Narlumidine complex by using different tools: (A, B) Zoomed-in and zoomed-out views of the NRF2– Narlumidine structure (C) Discovery Studio: Different types of interactions, polar (dark green lines) and hydrophobic analyze through Discovery studio; (D) Polar interactions shown by dark green lines through LIGPLOT+.

Online First Article

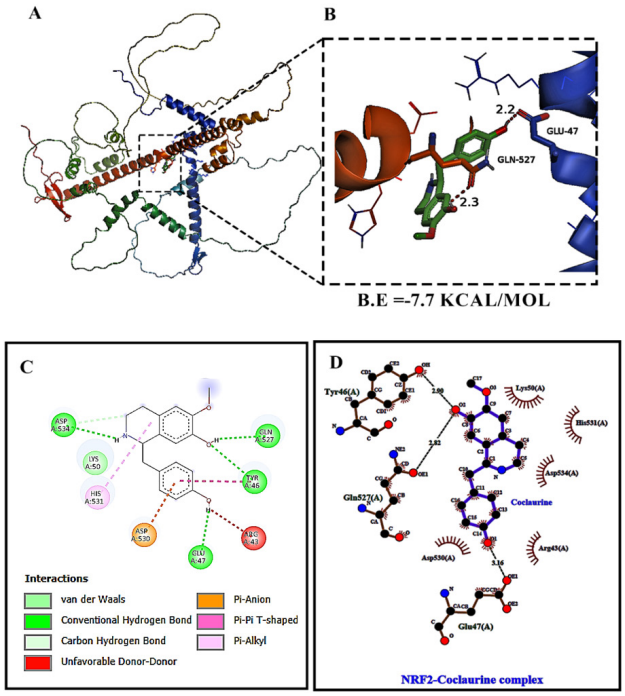


Fig. 4. Interaction analysis of NRF2-Coclaurine complex through different tools (A, B) Zoomed-in and zoomed-out views of the NRF2–Coclaurine complex structure (C) Discovery Studio: Different types of interactions, polar (dark green lines) and hydrophobic analyze through Discovery studio; (D) Polar interactions shown by dark green lines through LIGPLOT+.

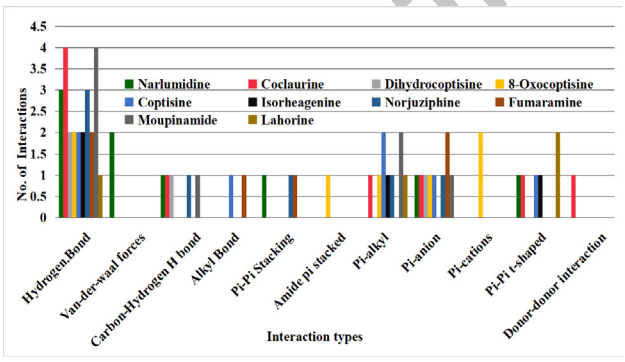


Fig. 5. Binding affinities and interaction patterns of *Fumaria indica*-derived compounds with NRF2.

(Supplementary Fig. S6). The interaction between NRF2 and fumaramine was also very stable; the complex formed hydrogen bonds with both ASP-530 and ARG-43 and Discovery Studio provided information on hydrophobic interactions of both the residues, all of which was validated by LigPlot+ Supplementary Fig. S7. Finally, in the NRF2-lahorine complex, only one hydrogen bond between LYS-53 and lahorine was observed in all the three analyses, even though Discovery Studio also detected other weak interactions such as pi-alkyl and pi-pi, indicating that the complex has a specific but rather weak binding (Supplementary Fig. S8). Comparative analysis of interactions for all the ten complexes has showed in the (Fig. 5).

Dynamic behavior of biomolecules and their ligand complexes

Molecular dynamics (MD) simulation is an indispensable tool for studying the dynamic behavior of biomolecules and their ligand complexes at atomic resolutions. MD simulation allows for a time-dependent assessment of the stability due to its flexibility, low cost and speed. GROMACS software were used as a virtual laboratory to examine the stability of some selected compounds. A molecular dynamics simulation of two complexes (narlumidine-NRF2 and coclaurine-NRF2) with 100 ns time-scale has been carried out guided by their docking studies, interaction mapping, drug-likeness properties etc. We analyzed several structural parameters, such as RMSD/RMSF/H. B/Rg.

Root mean square deviation (RMSD)

In order to compare the stability and conformational changes of the two complexes during the MD simulation, the RMSD of the backbone atoms was determined (Fig. 6A). From the RMSD (in Å) versus time (in ns) graph, which was obtained from the simulation results, it could be observed that both complexes remained at an RMSD of 0-3 Å for the first 70 ns of the MD simulation. However, there was a sudden change to 4. 54 Å in the NRF2-narlumidine complex at 70. 5 ns. The RMSD varied between 3-4. 59 Å in the range of 70-88. 9 ns and then was in the optimal range of 1. 7-3 Å in the range of 88. 9-100 ns. In the same manner, there was a sharp increase in RMSD in the NRF2-coclaurine complex after 70 ns. From 71. 68 to 89. 0 ns, RMSD was quite oscillatory and varied between 3. 1 to 8. 84 Å as depicted in the figure 6A (in red color). In the range of 89. 01–100 ns, the RMSD values varied from 1. 34 to 4. 60 Å.

The RMSD analysis of both complexes showed that the NRF2-narlumidine had a lower average RMSD value of about 1. 79 Å as compared to the NRF2-coclaurine complex which had an average RMSD value of about 2. 31 Å. As for the average RMSD values, they are all within the range of optimal RMSD (≤ 3.5 Å) (dos Santos Nascimento *et al*., 2024); however, to identify the reasons for the fluctuations observed, especially in the Coclaurine complex, additional analysis was carried out.

Online First Article

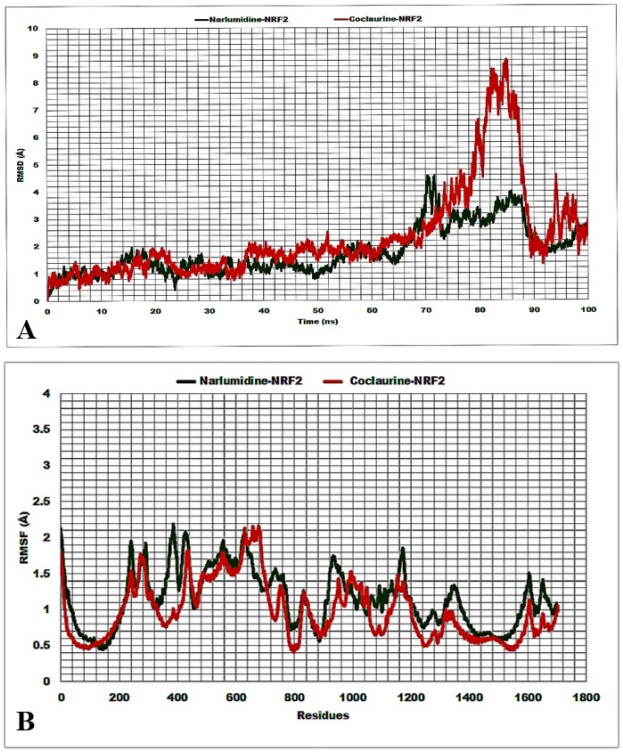


Fig. 6. RMSD (A) and RMSF (B) analysis of MD simulation results of NRF2-Narlumidine and NRF2-Coclaurine complexes.

Root mean square fluctuations (RMSF)

RMSF analysis is another parameter that is also used to determine the stability and the fluctuations that take place in protein-ligand complexes. The RMSF values were calculated for the NRF2-narlumidine (Green) and NRF2-coclaurine (Red) complexes as depicted in the (Fig. 6A). The average RMSF values for both complexes (NRF2-narlumidine: ~1. 18 Å, NRF2-coclaurine: ~0. 99 Å).

The graphical representation (Fig. 6B) shows the variation in the RMSF values of both the complexes in a more positive way over the residues. For all the 1800 residues examined, the RMSF values were observed to be within the range of 0. 413 Å to 2. 19 Å for both the complexes indicating that the binding conformation is well defined (Abedi-Karjiban *et al*., 2009).

Hydrogen bond dynamic

The dynamic analysis of hydrogen bond gives more information about the stability of the complexes. Protein-ligand complex's stability is significantly correlated with the number of hydrogen bonds (Fu *et al*., 2018). The number of hydrogen bonds formed during the simulation period of 100 ns is shown in the graph (Fig. 7A) for both the complexes. The outcomes of the current study revealed that the NRF2-narlumidine complex formed an average of approximately 51 hydrogen bonds while the NRF2-coclaurine complex formed an average of approximately 60 hydrogen bonds. The highest number of hydrogen bonds was 9 at 26.48ns in NRF2-coclaurine complex. This implies that coclaurine had more hydrogen bonding than narlumidine in the 100 ns time interval.

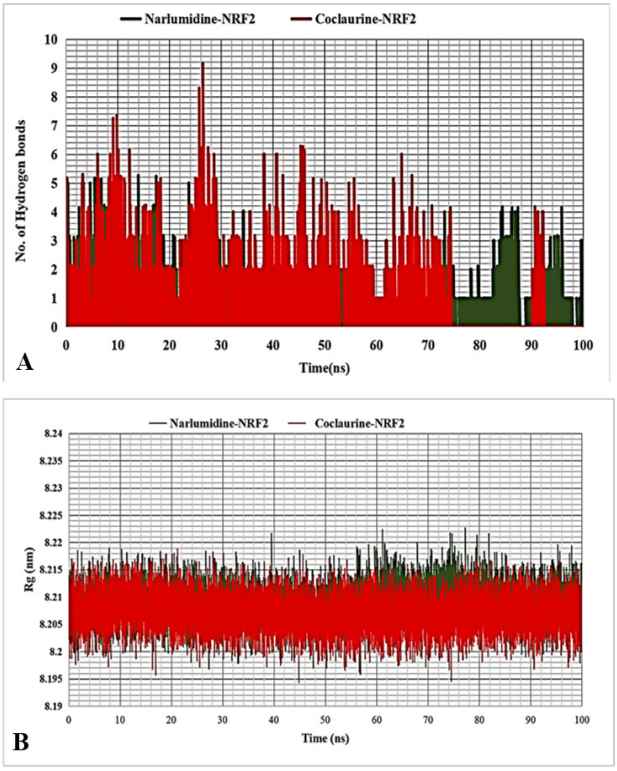


Fig. 7. Hydrogen bond dynamic (A) and radius of gyration analyses (B) of MD simulation results of NRF2-Narlumidine and NRF2-Coclaurine complexes.

Radius of gyration (Rg)

The radius of gyration (Rg) is used to describe the folding and unfolding of conformations or complexes. Rg values were estimated by the MD simulation in the time scale of 100 ns to determine the compaction level in the complexes (Lobanov *et al*., 2008). Small fluctuations in Rg values mean more compact and stable conformation (Gul *et al*., 2024).

The average radius of gyration (Rg) values of the complexes were approximately 8.209 nm for the NRF2–narlumidine complex and 8.207 nm for the NRF2–coclaurine complex. The highest Rg value was observed for the NRF2–narlumidine complex (8.222 nm at 70.36 ns), whereas the lowest Rg value was recorded for the NRF2–coclaurine complex (8.194 nm at 44.84 ns). The

Online First

Rg profiles showed no significant fluctuations throughout the 100 ns molecular dynamics simulation, indicating that both complexes maintained a stable and compact conformational structure during the simulation period (Gul *et al*., 2025).

Drug likeness analysis

All the drug likeness properties have been described as under.

Physicochemical characteristics

As shown in Table II**,** both compounds show drug-likeness and optimal molecular weight. Narlumidine has a greater density and rigidity (density: 1.044; rigid bonds: 26) as compared to coclaurine (density: 0.955; rigid bonds: 17) with comparable flexibilities. They have very low TPSA values (narlumidine 83.53 Å²; coclaurine 61.72 Å²) well below 140 Å² that discriminates membrane permeation. Both compounds pass the most important drug-likeness filters.

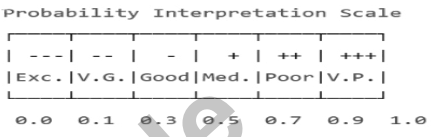
Table II. Physicochemical properties of narlumidine and coclaurine.

Property	Optimal values	Narlu-midine	Coclau-rine
MW	100-600	397.12	285.14
Volume	_	380.427	298.468
Density (MW/V)	_	1.044	0.955
No. of hydrogen bond acceptor	0-12	8	4
No. of hydrogen bond donor	0-7	0	3
No. of rotatable bonds	0-11	5	3
No. of ring	0-6	5	3
Maximum rings	0-18	12	10
No. of heteroatoms	1-15	8	4
Fraction of charged atoms	(-4) to (+4)	0	0
Number of rigid bonds	0-30	26	17
Flexibility (nRot/nRig)	_	0.192	0.176
Stereo centers	≤ 2	1	1
TPSA(Å²)	< 140	83.53	61.72
logS	_	-3.089	-2.591
logP	_	1.943	0.964
logD(Ph=7.4)	_	2.104	1.231
pka (Acid)	_	9.715	9.49
pka (Base)	_	8.628	7.223
Melting point (°C)	_	151.427	204.543
Boiling point (°C)	_	292.822	305.581

Tox21 pathway activation

As shown in Table III, coclaurine presented moderate activation of the aryl hydrocarbon receptor, estrogen receptor, and p53 which indicates partial involvement in pathways, whereas the narlumidine was mostly inactive and suppressed the p53 and the HSE elements slightly.

Table III. TOX21 Pathways, probability of activation for given nuclear receptors, probability is represented as:



Properties	Narlu-midine	Coclau-rine
Aryl hydrocarbon receptor	---	+
Androgen receptor	---	-
Androgen receptor ligand-binding domain	---	---
NR-aromatase	---	--
Estrogen receptor	---	+
Estrogen receptor ligand-binding domain	---	-
Peroxisome proliferator-activated receptor gamma	---	---
Antioxidant response element	---	+
ATPase family AAA domain containing 5	---	--
Heat shock element	-	-
Matrix metalloproteinase	---	++
Tumor suppressor protein p53	-	+

Medicinal properties

As presented in Table IV, a better drug-likeness was displayed by coclaurine with a QED score of 0.811 compared to 0.562. Both compounds met Lipinski, Pfizer, GSK and Golden Triangle criteria and also gave no PAINS alerts. A better global synthetic accessibility was exhibited by coclaurine which was more synthetically accessible. They both scored well enough in NP and promiscuity was moderate.

Toxicophore alerts

As shown in Table V, there were low structural warnings. That is, narlumidine experienced a few more warning flags (e.g., acute aquatic toxicity: 1; non-biodegradable: 1), compared to coclaurine which had zero of anything. The number of triggered 4 skin sensitization warnings and 1-2 FAF-Drugs4 rule violations triggered by both was equal.

Online First Article

Table IV. Enlisted various medicinal properties.

Property/Rule	Standard criteria	Narlumidine	Coclaurine
Quantitative estimate of drug-likeness	Attractive: > 0.67, Moderately Attractive: 0.49 - 0.67, Too Complex: < 0.34	0.562	0.811
Synthetic accessibility score	≥ 6=Difficult to synthesize, < 6 = Easy to synthesize	Easy	Easy
Global accessibility surface area	0 to 1= Difficult to synthesize, > 1=Easy to synthesize	Hard	Easy
Fraction of sp3 hybridized carbons	≥ 0.42	0.333	0.294
Molecular complexity estimate - 18	≥ 45	86.786	52.364
Natural product score	Range = -5 to +5, Npscore ∝ Probabilityof being a NP	0.547	1.365
Lipinski rule	Molecular weight < 500, LogP < 5, H-bond donors < 5, H-bond acceptors < 10	Accepted	Accepted
Pfizer rule	LogP > 3, TPSA< 75Å	Accepted	Accepted
GSK rule	MW ≤ 400, LogP ≤ 4	Accepted	Accepted
Golden triangle	MW= 200 - 500, Log p= (-2) - (5)	Accepted	Accepted
PAINS	480 Substructures	0	0
Alarm_NMR rule	Thiols reactive compounds	1	2
BMS rule	176 Substructures	0	0
Chelating rule	Chelating compounds	0	1
Colloidal aggregators	Excellent: p < 0.5, Moderate: P=0.5, Poor: p >0.5	0.164	0.519
FLuc inhibitors	Excellent: p < 0.5, Moderate: P=0.5, Poor: p >0.6	0.005	0.419
Blue fluorescence	Excellent: p < 0.5, Moderate: P=0.5, Poor: p >0.7	0.521	0.387
Green fluorescence	Excellent: p < 0.5, Moderate: P=0.5, Poor: p >0.8	0.306	0.371
Reactive compounds	Excellent: p < 0.5, Moderate: P=0.5, Poor: p >0.9	0.007	0.005
Promiscuous compounds	Excellent: p < 0.5, Moderate: P=0.5, Poor: p >0.10	0.463	0.203

Table V. Enlisted various Toxicophoric rules and status of compounds exhibiting any undesirable substructure.

Rule	Undesirable substructure	Narlumidine	Coclaurine
Acute aquatic toxicity rule	99	1	0
Genotoxic carcinogenicity mutagenicity rule	117	0	0
Nongenotoxic carcinogenicity rule	23	0	0
Skin sensitization rule	155	4	4
Aquatic toxicity rule	20	0	0
Nonbiodegradable	19	1	0
SureChEMBL rule	164	0	0
FAF-Drugs4 rule	154	2	1

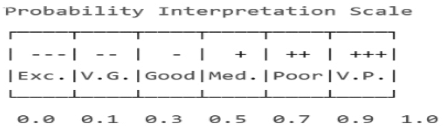
Online First Article

ADMET profile

As shown in Table VI, coclaurine has better oral bioavailability, with high values predicted to F20% F50%, even though it is a P-gp substrate thus, absorption can be interfered with. Narlumidine has low oral bioavailability predictions and non-interaction with P-gp. Caco-2 permeability of both compounds is acceptable and coclaurine has a lower plasma protein binding (66.7) than narlumidine (84.7), which would provide a greater amount of the free drug.

Narlumidine has high permeation through the BBB and this could be a drawback to targets outside of the CNS, whereas coclaurine does not pentrate the BBB. Coclaurine however appears to be flagged against OATP1B1, OATP1B3 and MRP1 inhibition, so there may be a transporter related drug interaction.

Table VI. ADME profile of the compounds where probability is represented as:



Absorption			
Property	**Optimal**	**Narlumidine**	**Coclaurine**
Caco-2 permeability (log unit)	> (-5.15)	-4.816	-5.119
MDCK permeability (Cm2/s)	low = < 2×10^{-6} Med. = (2 - 20) $\times10^{-6}$ High = >20×10^{-6}	-4.734	-4.786
PAMPA	_	-	--
Pgp inhibitor	_	---	---
Pgp substrate	_	---	+
HIA	_	---	---
F20%	_	---	++
F30%	_	---	+
F50%	_	---	+++
	DISTRIBUTION		
PPB	< 90%	84.70%	66.70%
VDss(L/kg)	0.04- 20	0.367	-0.296
BBB	_	+++	---
Fu	Low = < 5%, Middle = 5- 20 %, High = > 20%	17.00%	30.90%
OATP1B1 inhibitor	_	---	+++
OATP1B3 inhibitor	_	-	+++
BCRP inhibitor	_	---	--
MRP1 inhibitor	_	-	+++
BSEP inhibitor	_	+++	++
Metabolism			
CYP1A2 inhibitor	_	+++	---
CYP1A2 substrate	_	+++	+++
CYP2C19 inhibitor	_	+++	---
CYP2C19 substrate	_	+++	+
CYP2C9 inhibitor	_	-	---
CYP2C9 substrate	_	+++	-
CYP2D6 inhibitor	_	+++	+++
CYP2D6 substrate	_	+++	+++
CYP3A4 inhibitor	_	+++	---
CYP3A4 substrate	_	--	---
Property	**Optimal**	**Narlumidine**	**Coclaurine**
CYP2B6 inhibitor	_	--	---
CYP2B6 substrate	_	+++	---
CYP2C8 inhibitor	_	---	---
HLM Stability	_	---	+
	EXCRETION		
Plasma	High: > 15ml/min/kg, Mid.: 5-15ml/min/kg, Low: < 5ml/min/kg	4.214	6.705
T1/2 (Half-life)	Short = b/w 1-4 h, Ultra short = < 1 h, Intermediate:4-8 Long = >8	1.259	1.77

Table continues on next column.....

Table VII. Enlisted toxicity profile where parameters can be identified as: Excellent: p < 0.5, Moderate: P=0.5, Poor: p >0.5

Property (Unit)	Narlumidine	Coclaurine
hERG blockers (p)	0.673	0.531
hERG blockers (10um) (p)	0.787	0.658
DILI (p)	0.849	0.064
AMES toxicity (p)	0.606	0.452
Rat oral acute toxicity (p)	0.379	0.944
FDAMDD (p)	0.833	0.987
Skin sensitization (p)	0.996	0.664
Carcinogenicity (p)	0.854	0.041
Eye corrosion (p)	0.006	0.002
Eye irritation (p)	0.08	0.805
Respiratory (p)	0.836	0.983
Human hepatotoxicity (p)	0.788	0.836
Drug-induced nephrotoxicity (p)	0.91	0.384
Drug-induced neurotoxicity (p)	0.909	0.955
Ototoxicity (p)	0.524	0.155
Hematotoxicity (p)	0.582	0.019
Genotoxicity (p)	0.796	0.963
RPMI-8226 immunotoxicity (p)	0.137	0.034
A549 cytotoxicity (p)	0.12	0.312
Hek293 cytotoxicity (p)	0.272	0.344

Metabolically, narlumidine is a wide-ranged CYP inhibitor and substrate particularly of CYP 1A2, CYP 2C19, CYP 2D6 and CYP 3A4 which means that narlumidine has great metabolic liability. On the contrary, coclaurine exhibits little CYP inhibition and good hepatic microsomal stability.

Coclaurine exhibits clearance in the plasma (6.705

Online First Article

mL/min/kg) than narlumidine (4.214 mL/min/kg) as well as a prolonged half-life (1.77 h) than narlumidine (1.26 h). In general, coclaurine has a better ADME profile, but its transporter activity should be taken with caution. Table VII summarizes the predicted toxicity profile of narlumidine and coclaurine across different safety parameters. Both compounds showed favorable toxicity characteristics with low predicted risks for most endpoints. Although coclaurine displayed slightly higher toxicity probabilities for some parameters, the overall profile suggests acceptable safety potential for further experimental evaluation.

Radar plots have also been constructed for the physicochemical properties of top ten compounds has also been represented (Fig. 8). Alert structures for two top hit compounds on the basis of energy has also been showed in the Supplemenatry Figures S9, S10.

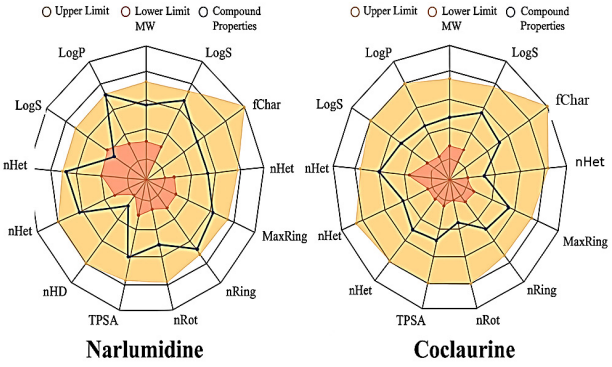


Fig. 8. Two Radar plots of two compounds, each labeled with their respective names, generated using ADMET Lab 02.

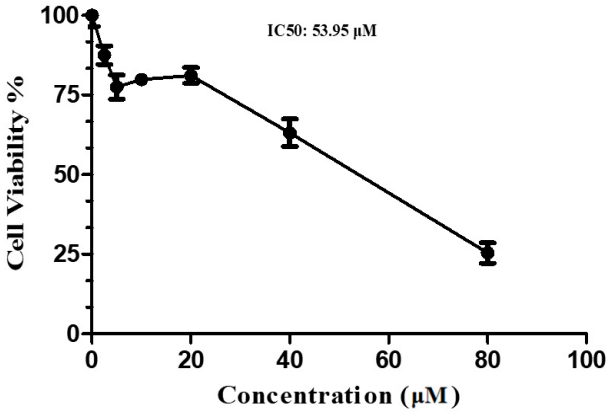


Fig. 9. Dose related toxicity of *Fumaria indica* (MTT assay). There was a decreased viability of cells associated with the increase of concentration (0 -100 µM) with an IC_{50} (53.95 µM/µl). Standard deviation is marked using error bars.

Anticancer activity of Fumaria indica *extract*

To assess the anticancer activity of *Fumaria indica* extract, MTT assay was employed. The data demonstrated that *Fumaria indica* extract inhibited the growth of MCF-7 cancer cells and reduced the viability in a dose-dependent manner with IC_{50} value approximately 53µM (Fig. 9).

DISCUSSION

In present study we have identified 10 bioactive molecules of *Fumaria indica*, as potential NRF2 inhibitors whose binding energies range from -7 to -8 kcal/mol. Using different filters and criteria including binding energy, Ki value, drug likeness and other physico-chemical properties, narlumidine and coclaurine were considered the most important and potential NRF2 inhibitors and were further characterized using MD-simmulation analysis.

The molecular docking results demonstrated that both narlumidine and coclaurine could bind to NEH1 and NEH2 domains of NRF2 through various types of binding interactions including stable hydrogen bonding and van der wall forces. The binding interactions of both compounds with NEH1 domain are of significant importance. The NEH1 domain contains the basic leucine zipper (bZIP) domain that is necessary to bind DNA and to form dimers with small Maf proteins to allow NRF2 to regulate the expression of antioxidant response element (ARE)-controlled genes. The presence of small molecules that bind to this domain can disrupt the transcriptional activity of NRF2 in knocking off DNA binding to reduce its activity in stimulating chemoresistance and tumor survival signaling (Zhang *et al*., 2007).

Conversely, NEH2 domain serves as a negative control domain which mediates the interaction of NRF2 with Keap1 via ETGE and DLG motifs, which targets NRF2 to ubiquitination and consequently proteasome degradation. Recognition by NEH2 can be disturbed by ligands binding within NEH2 to stabilize NRF2 and increase its cytoprotective activities or stabilize it to increase its degradation, as is the case with its interface (Tong *et al*., 2006). The dual binding of coclaurine to NEH1 and NEH2, therefore, indicates a two-way process, i.e., disruption of the NRF2 transcriptional apparatus at NEH1, and possible regulation of NRF2 stability at NEH2. On the other hand, combined NEH1xNEH2 interactions of narlumidine also reflect the possibility of a complex regulation process. Further study is suggested to explore the net result of binding of these two compounds on regulation of NRF2 transcriptional activity.

Narlumidine and coclaurine belong to the isoquinoline alkaloid family, a diverse group of nitrogen-containing natural products that includes compounds such

Online First Article

as berberine, palmatine, and sanguinarine. In fact, several members of this family have been reported to inhibit NRF2 activation and thereby suppressing growth of various cancer cells (Lu *et al*., 2020).

The physicochemical properties of the compounds were found to be good as indicated in the Table II. The physicochemical profile of narlumidine and coclaurine shows that both compounds lie within the optimal drug-like range, supporting their potential as lead drug candidates. Their molecular weights (397.12 Da and 285.14 Da) are favorable for oral bioavailability, while TPSA values below 140 Å² indicate good membrane permeability. Narlumidine is more lipophilic (logP 1.94) compared to coclaurine (0.96), whereas coclaurine has more hydrogen bond donors, suggesting stronger protein interactions. Both exhibit moderate flexibility and aromatic ring content, balancing rigidity with adaptability.

Nevertheless, different alert structures were recognized, and the two most significant compounds were narlumidine and coclaurine. These structures have their merits and demerits when it comes to cancer treatment. For instance, incorporation of furan rings improves bioactivity and chemical stability, which are important for therapy, but increases the potential toxicity due to metabolic reactivity, which is a problem for NRF2 modulation (Lu *et al*., 2020).The benzofuran moiety which is responsible for potent anticancer activity and selective cytotoxicity improves therapeutic efficacy but comes with the problems of electrophilicity and metabolic instability when it comes to selective NRF2 targeting. Also, the thiol group of narlumidine enhances its ability to bind covalently to target proteins and increases anticancer activity (Dalzoppo *et al*., 2017). However, thiol groups are very active, which causes side reactions and possible toxicity, which makes the problem of selective NRF2 inhibition more challenging (Bougoffa-Sadaoui *et al*., 2016). These properties must be optimized to enhance the therapeutic efficacy of narlumidine while reducing the toxicity associated with its use.

Another finding of this study was evaluation of anticancer activity of ethanolic extract of *Fumaria indica* in MCF-7 breast cancer cells. Ethanolic extract of *Fumaria indica* suppressed the growth of MCF-7 breast cancer cells with IC_{50} value approximately 53.95 µM after 24 h drug exposure. Our findings are in line with previously published reports in which anti-breast cancer potential of *Fumaria* species-derived alkaloids has been documented (Bougoffa-Sadaoui *et al*., 2016). Extracts of *Fumaria indica* have also shown a wide range of pharmacological effects such as antitumor value, which is possibly attributable to alkaloid/flavonoid components (Nasir *et al*., 2017).

CONCLUSION

In conclusion, we identified, 10 hit compounds as potential NRF2 inhibitors based on their binding energy. Interaction visualization and drug likeness properties further led to the selection of top two compounds; narlumidine and coclaurine which were subjected to virtual lab to further assess the molecular properties i.e. RMSF, RMSD, H.B and Rg. Out of these two compounds, narlumidine showed more satisfactory results as compared to coclaurine. However; further *in-vitro* and *in-vivo* studies are necessary to confirm the these *in-silico* findings to develp these molecules into potential NRF2 inhibitors.

DECLARATIONS

Acknowledgement

We thank Higher Education Commission (HEC) of Pakistan for providing funding for this study.

Funding

This study is supported by a research grant to Muhammad Khan from Higher Education Commission (HEC) of Pakistan (Grant No. 20-15729/NRPU/RandD/HEC/2021 2021).

Ethics approval consent to participate

Not applicable. This was an *in silico* and *in vitro* study that dealt only with cancerous cell lines and did not involve any human or animal subjects hence not requiring any ethical permission and informed consent.

Publication consent

Not applicable. It did not use the data of a particular person in any form (whole information, pictures, or films).

Data availability

All data generated or analyzed during this study are included in this published article and its supplementary information files. No additional datasets were generated or analyzed.

Supplementary material

There is supplementary material associated with this article. Access the material online at: https://dx.doi.org/10.17582/journal.pjz/20260421043057

Generative AI and AI assisted technology statement

The authors declare that no generative AI and AI assisted technology was used in the creation of this manuscript.

Online First Article

Statement of conflict of interest

The authors have declared no conflict of interest.

REFERENCES

Abedi-Karjiban, R., Abdul-Rahman, M.B., Basri, M., Salleh, A.B., Jacobs, D. and Abdul-Wahab, H., 2009. Molecular dynamics study of the structure, flexibility and dynamics of thermostable L1 lipase at high temperatures. *Protein J.,* **28**: 14-23.

Ackova, D.G., Maksimova, V., Smilkov, K., Buttari, B., Arese, M. and Saso, L., 2023. Alkaloids as natural NRF2 inhibitors: Chemoprevention and cytotoxic action in cancer. *Pharmaceuticals*, **16**: 850.

ADMET Lab 3, 2024. ADMETlab 3.0. Available from: https://admetlab3.scbdd.com/

Astuti, A.D. and Mutiara, A.B., 2009. Performance analysis on molecular dynamics simulation of protein using gromacs. *arXiv preprint*, arXiv: 0912.0893.

Banik, K., Khatoon, E., Harsha, C., Rana, V., Parama, D., Thakur, K.K. and Kunnumakkara, A.B. 2022. Wogonin and its analogs for the prevention and treatment of cancer: A systematic review. *Phytother. Res.*, **36**: 1854–1883.

Bellezza, G., Giambanco, I., Minelli, A. and Donato, R., 2018. Nrf2-Keap1 signaling in oxidative and reductive stress. *Biochim. Biophys. Acta Mol. Cell Res.*, **1865**: 721–733.

Bougoffa-Sadaoui, K., Gontier, E., Telliez, M.S., Lequart-Pillon, M., Ouadid-Ahidouch, H. and Maiza-Benabdesselam, F., 2016. Characterization of isoquinolin alkaloids from *Fumaria agraria* and evaluation of their antiproliferative activity against human breast cancer cell lines. *Phytothérapie*, **14**: 188–195.

Chowdhry, S., Zhang, Y., McMahon, M., Sutherland, C., Cuadrado, A. and Hayes, J., 2012. Nrf2 is controlled by two distinct β-TrCP recognition motifs in its Neh6 domain, one of which can be modulated by GSK-3 activity. *Oncogene*, **31**: 1–14.

Dalzoppo, D., Paolo, V. D., Calderan, L., Pasut, G., Rosato, A., Caccuri, A.M. and Quintieri, L., 2017. Thiol-activated anticancer agents: The state of the art. *Anticancer Agents Med. Chem.,* **17**: 4-20.

DeNicola, G.M., Karreth, F.A., Humpton, T.J., Gopinathan, A., Wei, C., Frese, K. and Tuveson, D.A., 2011. Oncogene-induced Nrf2 transcription promotes ROS detoxification and tumorigenesis. *Nature*, **475**: 106–109.

dos Santos Nascimento, I.J., Santana Gomes, J.N., de Oliveira Viana, J., de Medeiros e Silva, Y.M., Barbosa, E.G. and de Moura, R.O., 2024. The Power of molecular dynamics simulations and their applications to discover cysteine protease inhibitors. *Mini Rev. Med. Chem.*, **24**: 1125–1136.

George, M., Tharakan, M., Culberson, J., Reddy, A. and Reddy, P., 2022. Role of Nrf2 in aging, Alzheimer's and other neurodegenerative diseases. *Ageing Res. Rev.*, **82**: 101756.

Gilani, A.H., Bashir, S., Janbaz, K.H. and Khan, A., 2005. Pharmacological basis for the use of *Fumaria indica* in constipation and diarrhea. *J. Ethnopharmacol.*, **96**: 585–589.

GROMACS Development Team, 2024. *GROMACS 2024.0* (documentation and software download. GROMACS). https://manual.gromacs.org/documentation/2024.0/download.html.

Gul, S., Ali, M.A. and Khan, M., 2025. Brevilin a binds with Neh1 domain of NRF2 and inhibits its translocation into nucleus in cancer cells. *Pakistan J. Zool.,* **57**: 1925.

Gul, S., Muhammad, S., Irfan, M., Belali, T.M., Chaudhry, A.R. and Khan, M., 2024. Discovery of potential natural STAT3 inhibitors: An *in silico* molecular docking and molecular dynamics study. *J. Comput. Biophys. Chem.,* **23**: 189–205.

Hassan, S.H., Gul, S., Zahra, H.S., Maryam, A., Shakir, H.A., Khan, M. and Irfan, M., 2021. Alpha solanine: A novel natural bioactive molecule with anticancer effects in multiple human malignancies. *Nutr. Cancer,* **73**: 1541-1552.

Hayes, J.D. and Dinkova-Kostova, A.T., 2014. The Nrf2 regulatory network provides an interface between redox and intermediary metabolism. *Trends Biochem. Sci.,* **39**: 199-218.

IMPPAT, 2024. *Indian medicinal plants, phytochemistry and therapeutics*. Available from: https://cb.imsc.res.in/imppat/

Jaramillo, M.C. and Zhang, D.D., 2013. The emerging role of the Nrf2–Keap1 signaling pathway in cancer. *Genes Dev.,* **27**(20): 2179-2191.

Khan, M., Maryam, A., Qazi, J.I. and Ma, T., 2015. Targeting apoptosis and multiple signaling pathways with icariside II in cancer cells. *Int. J. biol. Sci.,* **11**: 1100.

Khan, M., Maryam, A., Zhang, H., Mehmood, T. and Ma, T., 2016. Killing cancer with platycodin D through multiple mechanisms. *J. Cell Mol. Med.,* **20**: 389-402.

Khan, M., Xiao, Y., Yu, B., Wang, N., Rasul, A., Yi, F. and Ma, T., 2012. Artabotryside A, a constituent from *Descurainia sophia* (L.) induces cell death in U87 glioma cells through apoptosis and cell cycle

Online First Article

arrest at G2/M phase. *J. Med. Pl. Res.,* **6**: 3754-3765.

Lobanov, M.Y., Bogatyreva, N.S. and Galzitskaya, O.V., 2008. Radius of gyration as an indicator of protein structure compactness. *Mol. Biol. (Mosk)*, **42**: 623-628.

Lu, D., Zhou, Y., Li, Q., Luo, J., Jiang, Q., He, B. and Tang, Q., 2020. Synthesis, *in vitro* antitumor activity and molecular mechanism of novel furan derivatives and their precursors. *Anticancer Agents Med. Chem*., **20**: 1475-1486.

Mehmood, T., Maryam, A., Tian, X., Khan, M. and Ma, T., 2017. Santamarine inhibits NF-κB and STAT3 activation and induces apoptosis in HepG2 liver cancer cells via oxidative stress. *J. Cancer,* **8**: 3707.

Nasir, B., Ahmad, M., Zahra, S.S., Fatima, H. and Ur-Rehman, T., 2017. Pharmacological evaluation of *Fumaria indica* (Hausskn.) Pugsley; a traditionally important medicinal plant. *Pakistan J. Bot.*, **49**: 119-132.

Sood, A., Mehrotra, A., Sharma, U., Aggarwal, D., Singh, T., Shahwan, M. and Kumar, M., 2024. Advancements and recent explorations of anti-cancer activity of chrysin: from molecular targets to therapeutic perspective. *Explore Target Anti-tumor Ther*., **5**: 477.

Tong, K.I., Katoh, Y., Kusunoki, H., Itoh, K., Tanaka, T. and Yamamoto, M., 2006. Keap1 recruits Neh2 through binding to ETGE and DLG motifs: characterization of the two-site molecular recognition model. *Mol. Cell Biol*., **26**: 2887-2900.

Zhang, J., Hosoya, T., Maruyama, A., Nishikawa, K., Maher, J.M., Ohta, T. and Yamamoto, M., 2007. Nrf2 Neh5 domain is differentially utilized in the transactivation of cytoprotective genes. *Biochem. J*., pp. 459-466. https://portlandpress.com/biochemj/article-abstract/404/3/459/41899/Nrf2-Neh5-domain-is-differentially-utilized-in-the

Zhang, J., Xu, H.X., Zhu, J.Q., Dou, Y.X., Xian, Y.F. and Lin, Z.X., 2023. Natural Nrf2 inhibitors: A review of their potential for cancer treatment. *Int. J. biol. Sci*., **19**: 3029–3046.

Online First Article